Thermal Modeling of EDM with Progression of Massive Random Electrical Discharges

J.F. Liu, Y.B. Guo[*]

Dept. of Mechanical Engineering, The University of Alabama, Tuscaloosa, AL 35487, USA
Tel.: +1 205 348 2615; E-mail address: yguo@eng.ua.edu

Abstract

Electrical discharge machining (EDM) is a competitive process to machine difficult-to-cut materials, but thermal damage is a critical concern for the EDMed parts. Finite element modeling provides insight into the thermal damage mechanism in EDM processes. However, current modeling approaches of an EDM process are limited to a single discharge, which is far from reality to predict thermal damage due to the accumulating effect of massive random. In this study, an innovative modeling approach to account for massive random discharges has been developed based on the stochastic EDM process and probability theory. Die sinking EDM of NiTi alloys was simulated to investigate the thermal damage mechanism with the progression of massive random discharges. The temperature history profiles of both top surface and subsurface showed pulsing characteristics with the progression of massive random discharges, which resulted from high-frequency random discharging phenomenon. A large temperature gradient was also found on the area below the top surface, while it gradually decreased in the deep subsurface. The predicted "coral reef" surface topography and uniform temperature distribution across the surface showed that the proposed model accounting for random discharge phenomenon proved to be an effective approach to investigate the effect of EDM processes.

Keywords: random discharge, EDM, stochastic process, finite element method, thermal damage

1 Introduction

1.1 EDM Background

Electrical discharge machining (EDM) is a competitive process to machine difficult-to-cut materials regardless of the strength. The contact free nature between a workpiece and an electrode enables the process free of burrs and chips. The low force in the EDM gap allows to machine high aspect ratio structures, complex parts geometry, and deep grooves with high accuracy. However, the

---

[*] Corresponding author
Tel.: 1-205-348-2615; fax: +1-205-348-6419. E-mail address: yguo@eng.ua.edu

thermal damage in EDM is a great concern that limits its broad applications. Several studies show the formation of thick and porous recast layers on the EDMed surfaces, which are induced from thermal damage (Kruth et al., 1995; Guo et al., 2013b). Although the thickness of recast layer can be significantly reduced with the development of "CleanCut" generator technology in EDM (Antar et al., 2012; Liu et al., 2014), the highly tensile residual stress is still detrimental to the fatigue life of EDMed components. Also, the thermal damage mechanism in both surface and subsurface remains unknown. Understanding the gap phenomena in EDM provides insight into the process mechanics and thermal damage evolutions. However, the transient process nature is difficult to analyse experimentally, while numerical modeling is an alternative method with great advantages in understanding the nonlinear transient dynamic process.

1.2   Finite Element Modeling of EDM

Finite element analysis is one of the effective methods to simulate the transient phenomenon of EDM. (Joshi & Pande, 2010) and (Murali & Yeo, 2005) used ANSYS to simulate the temperature field and obtained the geometry of a single discharge crater by removing the elements above the melting point. The simulated crater diameters matched the experimental results with reasonable errors. (Tao et al., 2012) simulated both the material melting phase and plasma collapsing phase using FLUENT, and the simulated crater geometry had a good agreement with the experimental result. (Guo et al., 2013a) programmed a DFLUX subroutine in ABAQUS to solve the long-time standing singularity issue of heat flux in finite element modeling of EDM, and simulated the temperature evolution of a discharge crater with discharge time. In addition, other simulation methods, including dynamic molecular simulation (Yang et al., 2011) and analytical modeling (Yeo et al., 2007; Mujumdar et al., 2014), were also used for the simulation of discharge crater geometries.

 However, all of previous modeling works are based on a single discharge. The thermal damages accumulated from massive discharges haven't been discussed yet. (Hinduja & Kunieda, 2013) point out that the process effects of multiple discharges need to be simulated sequentially instead of linearly superimposing the process effect of single discharge. However, the inherent random nature of discharging makes the discharge location unpredictable and challenging to simulate the EDM process at a macro level. As shown in Fig. 1, an electrical discharge always occurs in a random location instead of a deterministic region. A successful simulation of EDM processes is rooted in the determination of discharge locations. In the previous study (Morimoto & Kunieda, 2009), the random discharge location is predicted based on discharge delay time. (Morimoto & Kunieda, 2009) considers the discharge ignited at the location where there is a minimum discharge delay time, and successfully simulates twenty random electrical discharges and the resulting gap phenomenon. However, the large number of numerical iterations and many parameters to be determined in the model require tremendous computational resources to simulate massive random discharges. An efficient method is necessary to determine random discharge locations for the simulation of an EDM process.

1.3   Research Objectives

An insight on thermal damage mechanism of EDM with progression of massive random electrical discharges remains a challenging problem. The objectives of this study are to: (1) develop an innovative modeling approach to account for massive random discharge locations based on the stochastic process nature and probability theory; (2) investigate the temperature evolution and thermal damage mechanism with the progression of massive random discharges; (3) shed light on simulation of EDM processes at macro level.
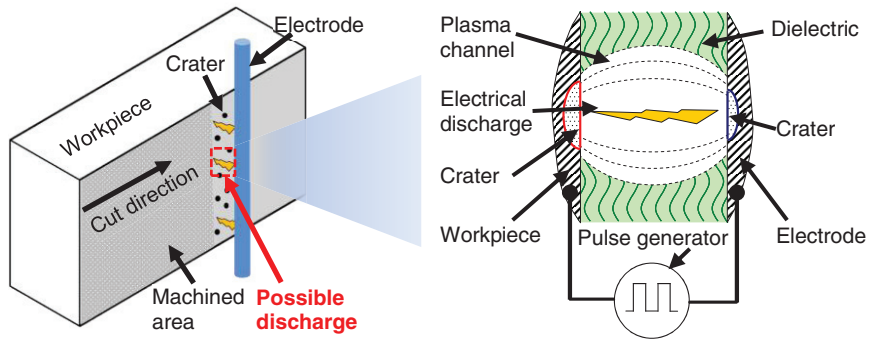
Fig. 1 Stochastic characteristics and process mechanism in wire-EDM.

2   Simulation Procedure of Die-Sinking EDM

2.1   Simulation Configurations

Model design and mesh

A 3D finite element model was used to simulate the die-sinking EDM of NiTi alloys. ABAQUS/standard was chosen for the simulation since the stochastic discharge location and time/space-dependent Gaussian heat flux can be only coded through the DFLUX subroutine in ABAQUS standard. Fig. 2 showed the 3D mesh of the model, which consisted of both 8-nodes and 4-nodes finite elements. The dimension of the model was developed as large as $2000 \times 2000 \times 400$ µm to accommodate enough electrical discharges and exhibit the stochastic nature. On the workpiece surface where the heat flux was applied, the model had the finest mesh ($4 \times 20 \times 20$ µm), which was able to provide a high resolution for spatial convergence. In this study, a heat transfer analysis was conducted to calculate the temperature field and thermal damage.

$$H(r,t) = \frac{C \times U \times I}{\pi R^2} e^{\left(-m\frac{r^2}{R^2}\right)}$$
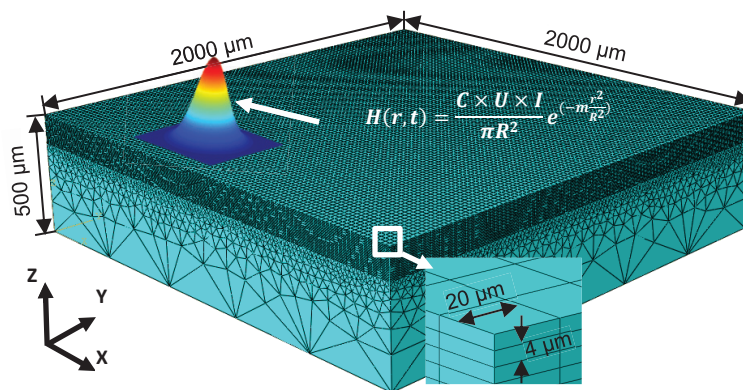
Fig. 2 3D FEM mesh for multiple random discharges.

A few assumptions were made for the simulation:
- Each discharge is ignited immediately, and discharge delay time is zero. Also, each electrical discharge has the same discharging intensity and discharging time.
- Heat flux of individual electrical discharge has a Gaussian distribution, which is a function of time and space.
- In the heat transfer analysis, heat conduction and convection are considered, while radiation is ignored.
- Material is considered to be removed when the temperature exceeds the melting point.
- Material properties are homogeneous and independent on temperature.

Initial and boundary conditions

In the heat transfer analysis, the initial temperature of the entire model was set to ambient temperature (20 °C). One boundary condition of heat convection was applied to the top surface to simulate the quenching effect from dielectrics. The coefficient of heat convection (*h*) was calculated as 1.2×10^4 W/m^{2}K based on laminar flow in Eq. 1 (Yunus, 2003).

$$h = \frac{k}{x} \times Nu_x \qquad (1)$$

where *h* was the coefficient of heat convection, the local distance (*x*) was chosen as an average value of 1mm based on the model size, thermal conductivity (*k*) of oil dielectric was set to 0.15 W/m·K, and Nusselt number (Nu_x) was set to 60 based on a flow rate of 1 m/s. No mechanical boundary condition was assigned since the model was free of stress and strain.

The other 4-side surfaces and the bottom surface of the model were also applied to heat convection ($h = 10^6$ W/m^{2}K) as boundary conditions to allow rapid heat dissipation through the model.

Simulation conditions and material properties

The simulation conditions were chosen based on a previous study of die-sinking EDM of NiTi alloys (Hsieh et al., 2013). Table 1 listed four EDM conditions with different discharge durations ranging from 3 µs to 50 µs. The discharge voltage (30 V) and discharge current (5 A) remain constant. A total of 1700 random discharges were simulated to capture the thermal damage evolution in the EDM process. Table 2 listed the physical properties of workpiece materials of NiTi alloys.

Table 1 Die-sinking EDM conditions

Case#	Discharge voltage U (V)	Discharge current I (A)	Pulse duration t_i (µs)	Pause duration t_o (µs)
1	30	5	3	3
2	30	5	12	12
3	30	5	25	25
4	30	5	50	50

Table 2 Physical properties of NiTi alloys

Density (Kg/m^3)	6500
Coefficient of thermal expansion (per °C)	11×10^{-6}
Thermal conductivity (W/m°C)	18
Specific heat (J/kg°C)	838
Melting temperature (°C)	1310

2.2   Modeling of Random Discharge Locations

Fig. 3 shows the modeling procedures of EDM processes with massive random discharges. The discharge location is determined by probability theory instead of discharge delay time. As reported by (Hinduja & Kunieda, 2013), an electrical discharge doesn't deterministically occur at the shortest gap between a workpiece and an electrode. A probabilistic method should be used to characterize the occurrence of a discharge instead of a deterministic way. Considering the stochastic nature of the electrical discharges, a mathematic model accounting for massive discharge locations is developed based on random coordinates as shown in Fig. 3. The location of a discharge (i) is determined by its 2D coordinate (x_i, y_i) shown in Eq. 2:

$$x_i = p_i \times L$$
$$y_i = q_i \times W$$

(2)

where (x_i, y_i) represents an arbitrary coordinate in Cartesian coordinate system, L is the sample length in x-axis, and W is the sample width in y-axis. p_i and q_i are the length ratio in their specific axis, which both have values between 0 and 1 independently. By randomly generating a value for p_i and q_i separately, the stochastic nature of a discharge (i) location can be described. Once massive random discharges occur, uniformly distributed discharge craters can be found on the machined surface.
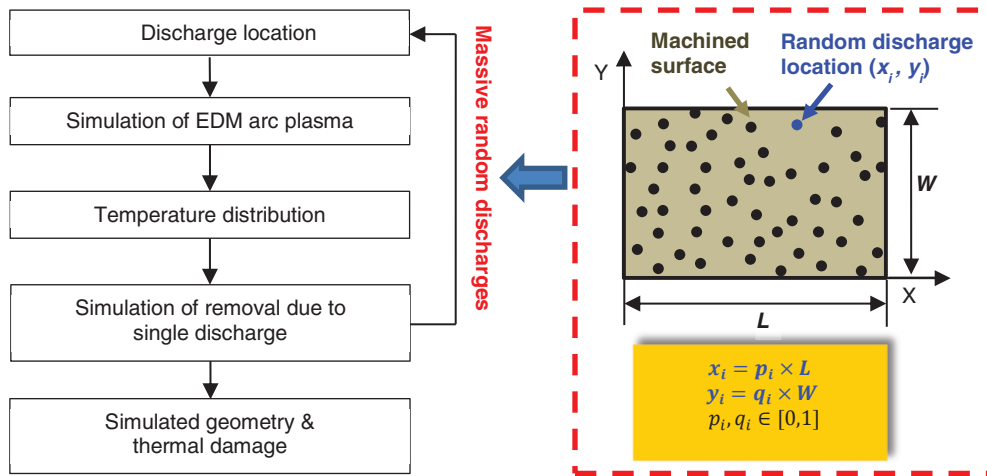

Fig. 3 Modeling procedure of EDM processes with massive random discharges.

2.3   Modeling of 3D Heat Flux

Gaussian distributed heat flux

In order to simulate the stochastic nature of multiple random discharges, heat flux modeling was performed in the following two steps. Firstly, the heat flux of a single electrical discharge was modelled as a function of discharge time and radial distance. The Gaussian heat flux was shown in Eq. 3:

$$H(r,t) = \frac{A \times U \times I}{\pi R(t)^2} \exp\left[-m \frac{r^2}{R(t)^2}\right]$$

(3)

where $H(r,t)$ is time/space-dependent heat flux, r is the radial distance from the plasma center, t is the discharge time, A is the fraction of plasma energy to the workpiece which is chosen as 18% in die-sinking EDM based on a previous study by (DiBitonto et al., 1989). Discharge voltage (U) and discharge current (I) are considered constant for each simulation condition, and shape coefficient of Gaussian curve (m) is set to 0.5. $R(t)$ is the time-dependent plasma radius, which is still a grand challenging to model. The detailed mathematical model of $R(t)$ will be discussed in the follow section.

The second step is to implement the single heat flux model to multiple electrical discharges simulation. The user subroutine DFLUX is programmed to apply the heat flux of a single discharge (Eq. 3) across the entire machined surface with the progression of massive random discharges. In each electrical discharge (i) period, it works by assigning a random coordinate (x_i, y_i) in Eqn. 2 as the plasma center, and then calculates the radial distance (r) to each node surrounding the plasma center by Eq. 4:

$$r = \sqrt{(x_{ni} - x_i)^2 + (y_{ni} - y_i)^2}$$ (4)

where (x_{ni}, y_{ni}) is the coordinate of the current node at each time increment during the simulation. Therefore, with a large amount of electrical discharges, the heat flux will be uniformly generated on the machined surface.

Modeling of plasma radius

Plasma radius is a critical factor that affects discharge crater geometry and temperature distribution. A successful simulation of EDM depends on a reliable and accurate plasma radius model. In the pass decades, it was believed that the arc plasma of EDM would keep expanding within the pulse duration until the plasma channel collapsed (DiBitonto et al., 1989; Patel et al., 1989). An empirical mathematic equation based on the continuously expanding model was widely used in the simulation of EDM (Guo et al., 2013a; Tao et al., 2012) as shown in Eq. 5:

$$R(t) = C \times t^{3/4} \quad (0 < t \leq t_i)$$ (5)

where $R(t)$ is the plasma radius, C is a constant expanding coefficient depending on EDM condition, t is the current discharge time and t_i is the pulse duration.

However, (Kojima et al., 2008; Natsu et al., 2006) recently reported a series of experimental results that contradicted to the theory of continuously expanding plasma. By characterizing the temperature distribution of arc plasma using optical emission spectroscopy, he demonstrated that the arc plasma didn't keep expanding during the entire pulse duration, but completed the expansion within a very short time after dielectric breaking down, and thereafter remained a constant radius. As a result, a new expansion model for plasma radius was proposed in this study as shown in Eq. 6:

$$R(t) = \begin{cases} C_1 \times t^{3/4} & (0 < t \leq t_c) \\ C_2 & (t_c < t \leq t_i) \end{cases}$$ (6)

where the plasma radius $R(t)$ expanded exponentially with current discharge time (t) within a critical time (t_c), and then remained a constant value (C_2) until the plasma channel collapsed after the pulse duration (t_i). However, the challenging of this model was to determine each coefficient, such as expanding coefficient (C_1), constant radius (C_2) and critical time (t_c). As pointed out by (Kojima et al., 2008), the stabilized plasma radius (C_2) depended on specific EDM conditions such as gap width and discharge current. Therefore, large amounts of experimental data were needed to quantify the plasma radius (C_2) as a function of EDM conditions. Another major factor, critical time (t_c), was also needed to be determined since it was affected by plasma expanding rate. In this simulation, considering the

EDM process was performed in an oil dielectric with the discharge current of 5 A, the stabilized plasma radius (C_2) was estimated as 120 µm, and critical time (t_c) as 100 µs based on the experimental data (Kojima et al., 2008). The expanding coefficient (C_1) was calculated as 0.12 by solving the boundary condition of Eq. 6. The new time-dependent plasma radius model was plotted in Fig. 4.
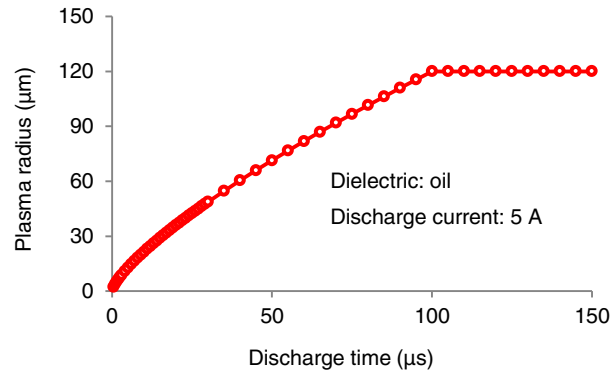

Fig. 4 Time-dependent plasma radius model.

3   Results and Discussions

3.1   Crater Geometry at a Single Discharge

The plasma radius model in Fig. 4 was implemented in ABAQUS by a DFLUX subroutine, and then preliminary simulations of a single electrical discharge were performed in order to validate the proposed heat flux model. Fig. 5 shows representative crater geometry after a single discharge of 50 µs. The depth-to-diameter ratio (δ) of the discharge crater is 0.19, which is much smaller than the one (0.4) obtained by a conventional plasma radius model in literature (Guo et al., 2013a). Considering most discharge craters in experiments showed a depth-to-diameter ratio (δ) of ~0.1 (Tao et al., 2012), the predicted discharge crater geometry in this study was significantly improved compared to the one predicted from the conventional plasma radius model. The difference between predicted geometry ($\delta = 0.19$) and experimental results ($\delta = ~0.1$) was because the re-solidification of molten materials was not considered in this simulation. The challenging to simulate the re-solidification process is to determine the fraction of molten materials which would solidify in the stochastic process, while no literature had reported those data yet.

In addition, Fig. 6 plotted discharge crater diameters with four different pulse durations for both simulated and experimental results. The predicted crater diameters showed a good agreement with experimental results. The prediction error was less than 30% in the pulse duration of 3 µs, and further decreased below 10% when longer pulse durations (12 µs, 25 µs and 50 µs) were simulated. The agreement between predicted crater diameters and experimental results validated the heat flux model of a single discharge, which could be used in multiple discharges simulation.
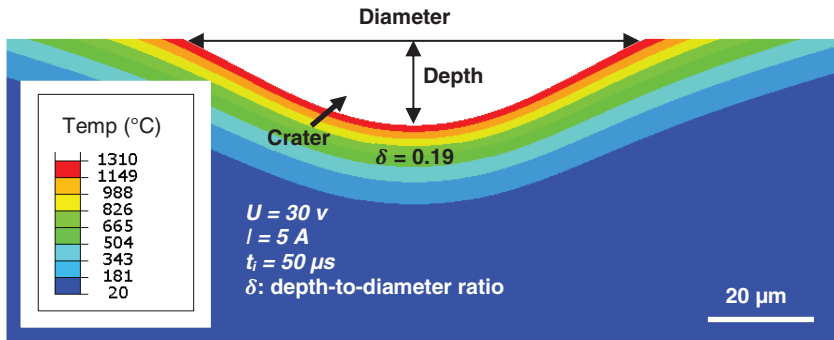
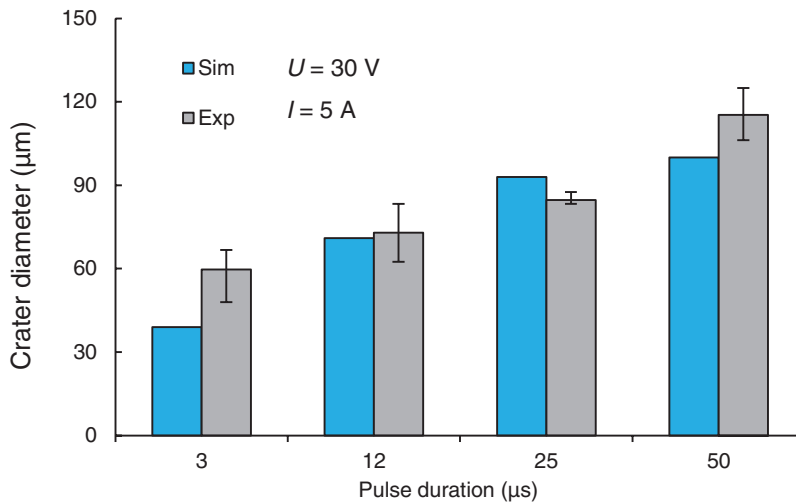Fig. 5 Crater geometry and temperature field after a single discharge.

Fig. 6 Discharge crater diameters with different pulse durations.

3.2 Locations of Massive Random Discharges

Fig. 7 showed the progression of 1700 random discharges with the pulse duration of 50 µs. The maximum temperature contour represented the highest temperature each node had ever reached during the 1700 random discharges. Each hot spot in the contour represented a discharge center. At the beginning of the process, 200 discharges randomly occurred on the surface with arbitrary locations. After that, more discharges occurred and spread across the entire surface after 500 discharges, but the distribution of the discharge locations were not uniform yet. After 1000 discharges, a uniform distribution of discharge locations was found on the surface. The discharge locations remained uniform after 1700 random discharges.
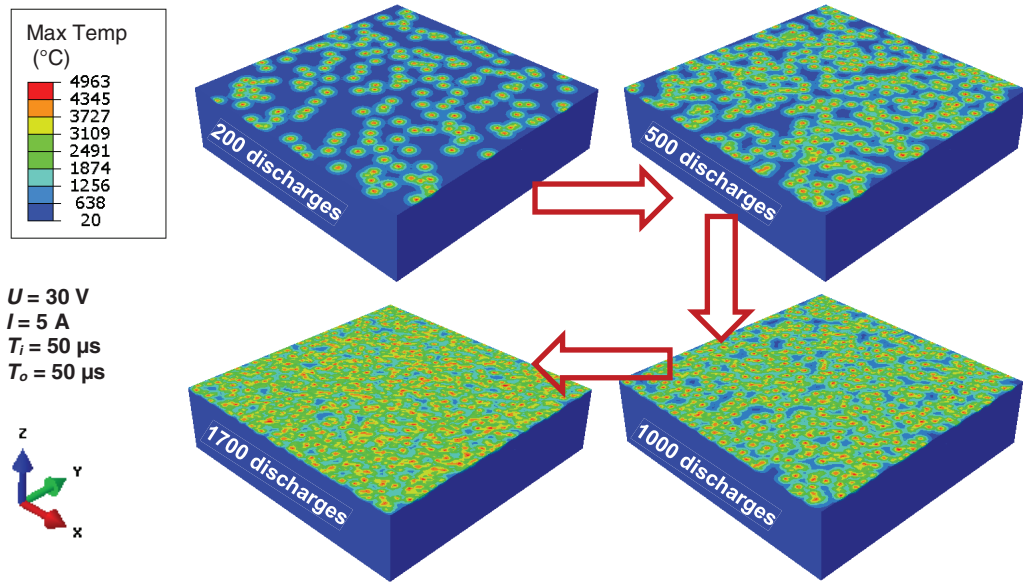
Fig. 7 Progression of massive random discharges.

3.3   Surface Topography and Temperature

Fig. 8 showed the evolution of surface topography within 1700 random discharges with the pulse duration of 50 µs. After 200 discharges, the surface was partially eroded and characterized by randomly distributed discharge craters. Most of the craters at this stage remained semispherical geometry. After 500 discharges, most of the surface was eroded, while a trace of areas were still free of thermal damage. When the discharge occurred 1000 times, the entire surface was eroded. Irregular craters instead of semispherical craters were observed on the machined surface due to excessive overlaps of discharge craters. Peak-to-valley distance (~50 µm) of the machined surface was larger than the depth of a single discharge crater (~20 µm). A similar phenomenon was observed on the machined surface after 1700 discharges, while the peak-to-valley distance increased to ~70 µm.

Fig. 9 showed the temperature evolution of 5 specific locations on the machined surface within 1700 discharges (L1 represented the central location, and L2 - L5, respectively, was the center of the path from L1 to each corner of the model). Each temperature profile showed a pulsing nature with varying amplitudes, which corresponded to the high-frequency discharging phenomenon in the EDM process. For example, each temperature spike in the profile of central location (L1) represented a heating/cooling cycle caused by an electrical discharge, and the magnitude of each temperature spike depended on the radial distance between L1 and each discharge center. The location of L1 would have a higher temperature spike when a discharge occurred near the center of the model, while it would have a lower temperature spike when a discharge happened far away from L1. The temperature evolution of other locations (L2 – L5) had the similar pulsing nature. Also, the average temperature and standard deviation of the temperature for each location within 1700 discharges had similar values, indicating that the thermal damage caused to the machined surface was uniform.
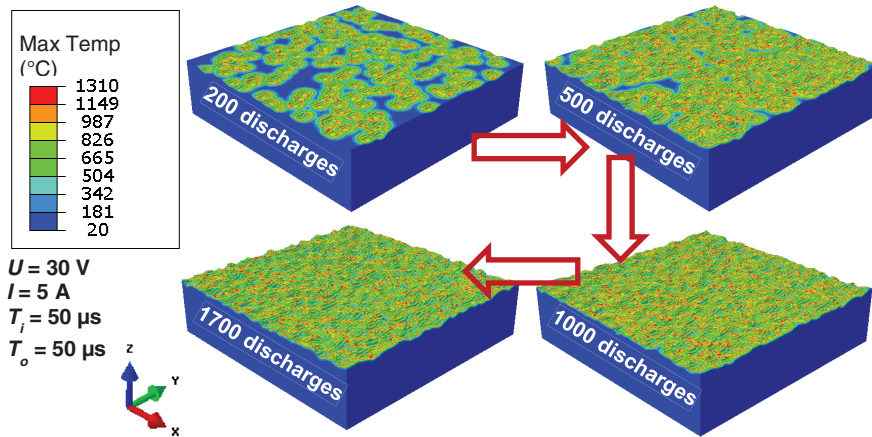
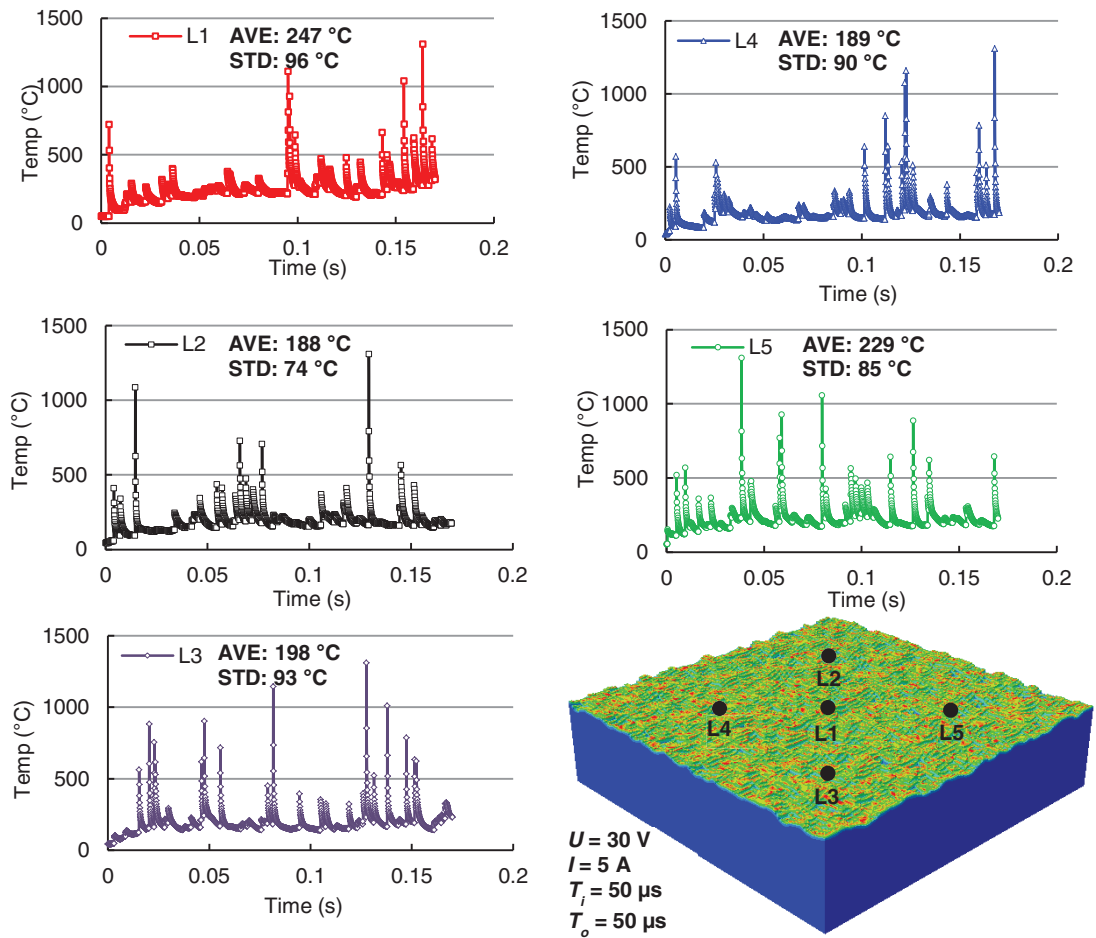Fig. 8 Evolution of surface topography in die-sinking EDM.

Fig. 9 Temperature evolution of different locations on the machined surface.

3.4   Thermal Damage in the Subsurface

Fig. 10 showed the cross section profile of the EDMed model after 1700 discharges, and the temperature evolution in the subsurface. Non-uniform discharge craters were found in the subsurface, which was due to the overlaps of multiple discharge craters. A similar irregular profile in the cross section was also observed in previous experiments (Liu et al., 2014; Klink et al., 2011). In addition, the temperature history of node 1 (top surface) and node 2 (in the depth of 20 µm) were plotted in Fig. 10. The temperature evolution of node 2 in the subsurface showed a similar pulsing characteristic with that of node 1 on the top surface. The temperature spikes of the both profiles occurred synchronously, while the temperature magnitude of node 2 was much smaller than that of node 1, indicating a large thermal gradient from a top surface to its subsurface.

Fig. 11 showed the maximum temperature profile in the subsurface after 1700 discharges. All of the three paths in the subsurface showed a similar temperature profile, indicating a uniform thermal damage across the model. Within the depth of ~ 20 µm, a large temperature gradient was found and the maximum temperature decreased significantly from ~ 1300 °C to ~300 °C. However, in a deeper area of ~ 20 - 80 µm, the temperature gradient was small and the temperature slightly dropped from ~ 300 °C to ~ 100 °C.
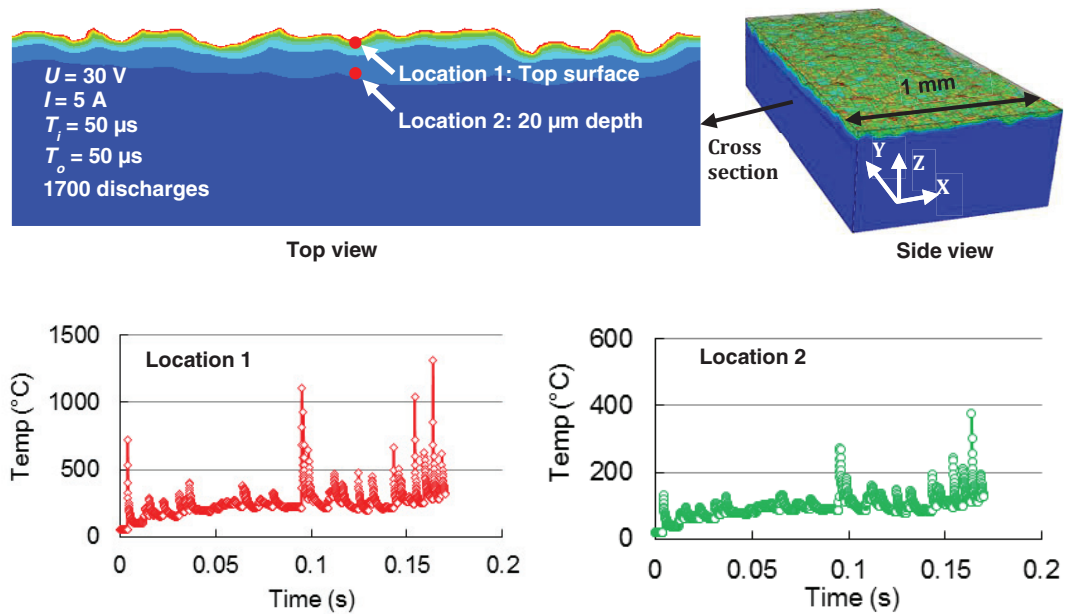

Fig. 10 Cross section profile and temperature evolution in the subsurface.
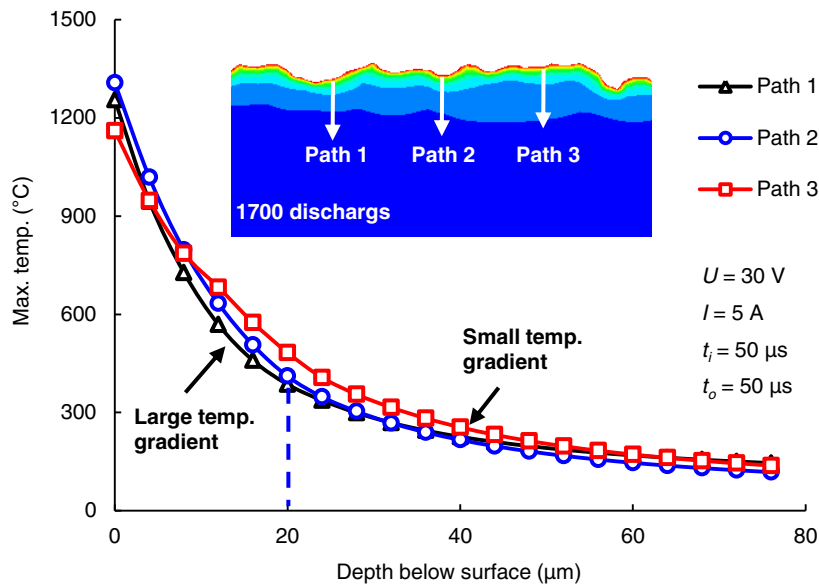
Fig. 11 Maximum temperature profile in the subsurface.

4 Conclusions

In this study, an innovative modeling approach was developed to account for massive random discharge locations based on the stochastic process nature and probability theory. A die-sinking EDM of NiTi alloys was simulated at a macro level. The key findings are as follow:

- An innovative model accounting for random discharge phenomenon was successfully implemented in ABAQUS to simulate massive random discharges. The massive random discharges generated an isotropic surface.
- The predicted crater geometry of a single discharge agrees with experimental results very well.
- The evolution of surface topography and temperature with 1700 discharges was characterized. The temperature history of the top surface showed a pulsing nature, which resulted from high-frequency random discharging phenomenon.
- The subsurface showed a larger temperature gradient within the depth of ∼ 20 µm, while a smaller temperature gradient in the deep subsurface.
- The proposed model accounting for random discharge phenomenon proved to be an effective approach to investigate the effect of EDM process.

Acknowledgement

References

Antar, M. T., Soo, S. L., Aspinwall, D. K., Sage, C., Cuttell, M., Perez, R., Winn, A. J. (2012). Fatigue response of Udimet 720 following minimum damage wire electrical discharge machining, *Materials & Design,* 42, 295-300.

DiBitonto, D. D., Eubank, P. T., Patel, M. R., Barrufet, M. A. (1989). Theoretical models of the electrical discharge machining process. I. A simple cathode erosion model, *Journal of Applied Physics,* 66(9), 4095-4103.

Guo, Y. B., Klink, A., Klocke, F. (2013a). Multiscale modeling of sinking-EDM with Gaussian heat flux via user subroutine, *Procedia CIRP,* 6(0), 438-443.

Guo, Y., Klink, A., Fu, C., Snyder, J. (2013b). Machinability and surface integrity of nitinol shape memory alloy, *CIRP Annals - Manufacturing Technology,* 62(1), 83-86.

Hinduja, S., Kunieda, M. (2013). Modelling of ECM and EDM processes, *CIRP Annals - Manufacturing Technology,* 62(2), 775-797.

Hsieh, S. F., Hsue, A. W. J., Chen, S. L., Lin, M. H., Ou, K. L., Mao, P. L. (2013). EDM surface characteristics and shape recovery ability of $ti_{35.5}ni_{48.5}zr_{16}$ and $ni_{60}al_{24.5}fe_{15.5}$ ternary shape memory alloys, *Journal of Alloys and Compounds,* 571(0), 63-68.

Joshi, S. N., Pande, S. S. (2010). Thermo-physical modeling of die-sinking edm process, *Journal of Manufacturing Processes,* 12(1), 45-56.

Klink, A., Guo, Y. B., Klocke, F. (2011). Surface Integrity evolution of powder metallurgical tool steel by main cut and finishing trim cuts in wire-EDM, *Procedia Engineering,* 19(0), 178-183.

Kojima, A., Natsu, W., Kunieda, M. (2008). Spectroscopic measurement of arc plasma diameter in EDM, *CIRP Annals - Manufacturing Technology,* 57(1), 203-207.

Kruth, J. -., Stevens, L., Froyen, L., Lauwers, B. (1995). Study of the white layer of a surface machined by die-sinking electro-discharge machining, *CIRP Annals - Manufacturing Technology,* 44(1), 169-172.

Liu, J., Li, L., Guo, Y. (2014). Surface Integrity evolution from main cut mode to finish trim cut mode in w-edm of shape memory alloy, *Applied Surface Science,* 308 253-260.

Morimoto, K., Kunieda, M. (2009). Sinking EDM simulation by determining discharge locations based on discharge delay time, *CIRP Annals - Manufacturing Technology,* 58(1), 221-224.

Mujumdar, S. S., Curreli, D., Kapoor, S. G., Ruzic, D. (2014). Modeling of Melt-pool formation and material removal in micro electro-discharge machining, *Journal of Manufacturing Science and Engineering*, 137(3), 031007.

Murali, M. S., Yeo, S. (2005). Process simulation and residual stress estimation of micro- electro discharge machining using finite element method, *Japanese Journal of Applied Physics,* 44, 5254.

Natsu, W., Shimoyamada, M., Kunieda, M. (2006). Study on expansion process of edm arc plasma, *JSME* International *Journal Series C,* 49(2), 600-605.

Patel, M. R., Barrufet, M. A., Eubank, P. T., DiBitonto, D. D. (1989). Theoretical models of the electrical discharge machining process. II. the Anode erosion model, *Journal of Applied Physics,* 66(9), 4104-4111.

Tao, J., Ni, J., Shih, A. J. (2012). Modeling of the anode crater formation in electrical discharge machining, *Ann Arbor,* 1001 48109.

Yang, X., Guo, J., Chen, X., Kunieda, M. (2011). Molecular dynamics simulation of the material removal mechanism in micro-EDM, *Precision Engineering,* 35(1), 51-57.

Yeo, S., Kurnia, W., Tan, P. (2007). Electro-thermal modelling of anode and cathode in micro-EDM, *Journal of Physics D: Applied Physics,* 40(8), 2513.

Yunus, A. C. (2003). Heat transfer: A Practical Approach, *MacGraw-Hill,.*